Rare-Earth Metals (REMs) in Nickel Aluminide–Based Alloys: II. Effect of a REM on the Phase Composition of a Multicomponent Ni_3Al-Based Alloy

K. B. Povarova[a], A. A. Drozdov[a], N. K. Kazanskaya[a], A. E. Morozov[a], Yu. R. Kolobov[b], T. N. Vershinina[b], and E. V. Kozlov[c]

[a] *Baikov Institute of Metallurgy and Materials Science, Leninskii pr. 49, Moscow, 119991 Russia*
e-mail: povarova@imet.ac.ru
[b] *BelGU, Belgorod, Russia*
[c] *Tomsk State Architectural and Building University, Tomsk, Russia*

Abstract—The hardening mechanisms are studied in the cast high-temperature next-generation materials that are based on the intermetallic compound Ni_3Al and are low alloyed with refractory (W, Re, Mo, Cr) and reaction- and surface-active (REM, Ti, etc.) metals. The interaction of the main impurities (C, O, Si, S) with three characteristic representatives of the REM group (namely, Y, La, Ce), which can be used for alloying, is analyzed. The reported data on the behavior of some REMs in the alloys based on nickel monoaluminide NiAl are considered. The effect of the REMs on the phase compositions of real multicomponent semicommercial Ni_3Al-based VKNA alloys produced by directional solidification is investigated, and the excess phases precipitating upon alloying are revealed. Alloying with refractory metals and REMs is shown to lead to the formation of nanophases that stabilize the dendritic or single-crystal structure of VKNA-type cast alloys and strengthen the interface boundaries in them.

INTRODUCTION

Based on the data in [1–3], we can state that γ'-Ni_3Al-based $\gamma' + \gamma$ alloys, including complexly alloyed nickel-based alloys with 85–90 vol % γ solid solution, represent natural eutectic composite materials (CMs). The structure that is self-organized during solidification has a very high thermal stability up to near-melting temperatures. The structure of such alloys forms according to at least the following three mechanisms, which are used to strengthen $\gamma' + \gamma$ nickel superalloys: (i) the creation of a heterophase structure with an optimum misfit, (ii) solid-solution hardening of the γ' and γ phases by the main alloying elements (Cr, Ti, Mo, W, Hf, Zr, Fe, Co), and (iii) the formation of metallographic and crystallographic textures and a decrease in the length of transverse grain boundaries using directional solidification (DS). The last mechanism increases the creep resistance, the long-term strength, and the lifetime at working temperatures. Moreover, the following three additional mechanisms, which are not realized in nickel superalloys and are realized in Ni_3Al-based cast alloys, can be involved to increase the strength and lifetime: (iv) the additional hardening of γ-phase inclusions in the eutectic dendrites in γ'-Ni_3Al-based cast alloys due to the precipitation of high-temperature disperse γ'_{sec} particles in the γ inclusions, (v) the formation of a microstructure and hardening that are similar to those in natural CMs and are caused by dendritic segregation during DS[1], and (vi) additional hardening and stabilization of the structure of a natural $\gamma' + \gamma$ CM by the nanoparticles of the hard phases that have a complex ordered crystal lattice based on refractory metals (W, Re, Mo, Cr) and high- and surface-active alloying elements (AEs) and are in equilibrium with the $\gamma' + \gamma$ phases. These AEs involve Group III transition metals, including rare-earth metals (REMs), where REM = Sc, Y, La, and lanthanides.

In the first part of this work [4], we studied the physicochemical interaction in the Ni–Al–REM systems and the interaction of some REMs (REM = Y, La, Ce)

[1] The AEs introduced into the alloys are distributed between dendrite arms and the interarm space in the γ' and γ phases during solidification. The distribution of low-melting-point and refractory AEs and active and surface-active AEs in all cast DS alloys is always nonequilibrium. The degree of approaching an equilibrium AE distribution depends on the solubility of AEs in the γ' and γ phases, the degree of homogenization of the melt of a cast alloy before solidification (high-temperature processing of the melt, the method of introducing AEs into the alloy, the interaction between AEs and impurities inherent in real alloys), solidification conditions, and so on.

with the main AEs in nickel aluminide–based alloys (Ti (Zr, Hf), Cr (Mo, W)). An analysis of the binary REM–Ni (Al, AE) phase diagrams demonstrates that stable binary compounds with nickel and aluminum can form in these systems. However, according to the well-known ternary Ni–Al–*R* (*R* = REM) phase diagrams, these binary REM aluminides or nickelides are not in equilibrium with nickel aluminides, since the field between them is closed by the extended regions of RAl_xNi_{5-x}-type solid solutions of aluminum in RNi_5, in which aluminum substitutes for nickel in spite of the difference in their electrochemical properties (because their atomic sizes are significantly smaller than those of REMs). In the binary systems of REMs with the AEs listed above, no intermetallic compounds form, some systems exhibit immiscibility in the liquid state (melt separation), and mutual solubility in the solid state is almost absent (is present at an impurity level) [4].

Since the atomic radii of REMs are significantly larger than those of aluminum and nickel, REMs do not dissolve in solid solutions based on nickel aluminides (γ'-Ni_3Al, NiAl) and γ-Ni. Being surface-active metals, REMs should be localized in defect regions in a structure, namely, various boundaries, interfaces, interarm space, and so on, which can result in the formation of excess phases with both nickel, aluminum, and impurity elements. Because of their surface-active properties, REMs should affect the nucleation and growth of crystals during solidification and should decrease the surface tension of the liquid metal and the energy of grain nucleation. As a result, the number of grains should increase, which refines the microstructure and, in turn, affects the mechanical properties.

In the second part of the work, we study the effect of REMs on the phase composition of real DS multicomponent semicommercial VKNA alloys based on Ni_3Al and containing REMs and various impurities, which can also interact with the REMs. C, O, Si, and S are known to be the main impurities in these Ni_3Al-based alloys whose interaction with REMs should be taken into account. Therefore, the purpose of this work is to analyze the interaction of these impurities with three characteristic representative of the REM group, which can be used for alloying; to consider the reported data on the behavior of some REMs in alloys based on nickel monoaluminide; and to experimentally study the effect of REMs on the phase composition, structure, and properties of VKNA-type Ni_3Al-based alloys.

Interaction of REMs (Y, La, Ce) with Impurity Elements

When REMs are introduced into Ni_3Al-based alloys, we can expect the fixation of carbon, silicon, oxygen, and sulfur into refractory carbides, silicides, oxides, and sulfides, which can form disperse hardening-phase (predominantly, carbides and silicides) particles or coarse spherical particles, which are weakly related to a matrix structure. This assumption is based on the formation of the following series of refractory compounds:

Carbides. Y_3C, $Y_{15}C_{19}$, Y_2C_3, YC_2 [5–7]; LaC_2 (T_m = 2235°C, including α-LaC_2 with the CaC_2 crystal lattice and the *tI*6 structure type and β-LaC_2 with the CaF_2 crystal lattice and the *cF*12 structure type); La_2C_3 (Pu_2C_3 crystal lattice, *cI*40 structure type; it forms according to a peritectic reaction at 1415°C); CeC_2 (T_m = 2340°C, including α-CeC_2 with the CaC_2 crystal lattice and the *tI*6 structure type and β-CeC_2 with the CaF_2 crystal lattice and the *tI*16 structure type); Ce_2C_3 (Pu_2C_3 crystal lattice, *cI*40 structure type; it forms according to a peritectic reaction at 1537°C)[2].

Silicides. Y_5Si_3 (Mn_5Si_3 crystal lattice, *hP*16 structure type), Y_5Si_4 (Y_5Si_4 crystal lattice, *oP*36 structure type), YSi (CrB crystal lattice, *oC*8 structure type), and Y_3Si_5 (AlB_2 crystal lattice, *hP*3 structure type), of which only Y_5Si_3 melts congruently at 1875°C; La_5Si_3 (Cr_5B_3 crystal lattice, *tI*32 structure type), La_3Si_2 (U_3Si_2 crystal lattice, *tP*10 structure type), La_5Si_4 (Zr_5Si_4 crystal lattice, *tP*36 structure type), LaSi (FeB crystal lattice, *oP*8 structure type), $LaSi_2$ ($ThSi_2$ crystal lattice, *tI*12 structure type), and $LaSi_{1.65}$ ($GdSi_2$ crystal lattice) [8]; Ce_5Si_3 (T_m = 1400°C, W_5Si_3 or Cr_5B_2 crystal lattice, *tI*32 structure type), Ce_3Si_2 (T_m = 1390°C, U_3Si_2 crystal lattice, *tP*10 structure type), Ce_5Si_4 (T_m = 1440°C, Zr_5Si_4 crystal lattice, *tP*36 structure type), CeSi (T_m = 1470°C, FeB crystal lattice, *oP*8 structure type), Ce_3Si_5 (T_m = 1560°C, α-$GdSi_2$ crystal lattice, *oI*12 structure type), and $CeSi_2$ (T_m = 1620°C, α-$ThSi_2$ crystal lattice, *tI*12 structure type) [7, 9].

Oxides. Y_2O_3 (T_m = 2458°C; high-temperature modification with the Mn_2O_3 crystal lattice and the *cI*80 structure type; monoclinic modification with the Sm_2O_3 crystal lattice and the *mC*30 structure type; at 2330°C, La_2O_3-type hexagonal modification with *hP*5 structure type) forms a eutectic with the β-Y solid solution at 1560°C and 37.4 at % O [7]; La_2O_3 (T_m = 2210°C; at 450–550°C, bcc structure, Mn_2O_3 crystal lattice, *cI*80 structure type; at 550°C, hexagonal structure) [7, 10]; Ce_2O_3, $CeO_{2.714}$ (δ), $CeO_{2.778}$ (γ), $CeO_{1.800}$, $CeO_{1.818}$ (β), CeO_2, and CeO [7].

Sulfides. YS (T_m = 2060°C, NaCl cubic lattice), Y_5S_7 (T_m = 1630°C), and Y_2S_3 (T_m = 1660°C) [7]; LaS (T_m = 2175°C), La_3S_4 (T_m = 2115°C), La_2S_3 (T_m = 1650°C), and LaS_2 (T_m = 1650°C) [11]; CeS (T_m = 2450°C), Ce_3S_4 (T_m = 2050°C), Ce_2S_3 (T_m = 1890°C), CeS_2 (T_m = 1700°C), and Ce_5S_7 (T_m = 1450°C) [12].

Neodymium in a NiAl-based Multicomponent Alloy

The study of the effect of neodymium additions (0, 0.005, 0.05, 0.1, 0.5 wt %) on the microstructure and mechanical properties of the cast eutectic (at %) NiAl–

[2] O. V. Gardiichuk, "Binary Phase Diagrams of Rare-Earth Metals with Carbon (Sc–C, La–C, Ce–C, Pr–C)," *Extended Abstract of Cand. Sci. (Chem.) Dissertation*, Kiev, 1967.

Compositions of the base alloys

Alloy	Element content, wt %									
	Ni	Al	Cr	W	Mo	Ti	Co	La	Re	C
1	Base	8.0–9.0	5.0–6.0	2.0–4.0	2.5–5.5	0.6–2.0	–	0.0015	–	0.02–0.08
2	Base	8.1–8.6	5.6–6.0	2.5–3.5	4.5–5.5	0.3–0.7	4.0–5.0	≤0.002	1.2–1.6	0.01–0.05

28Cr–5.5Mo–0.5Hf alloy demonstrates the following [13]. Neodymium effectively decreases the oxygen content from 0.011 to 0.0026–0.0033 wt %, does not affect the sulfur content (0.003 wt %), refines the structure, and changes the phase composition of this complexly alloyed alloy. When more than 0.1 wt % Nd is introduced, Nd_2Ni_{17} inclusions appear at the NiAl/Cr(Mo) interface apart from NiAl, the lamellar phase Cr(Mo), and randomly distributed Ni_2AlHf inclusions. No Nd_2O_3 inclusions are detected in spite of the fact that R_2O_3-type oxides form in Ni, Ti, and TiAl alloys with an REM. Samples alloyed with 0.05 wt % Nd have the best combination of strength and plasticity during compression tests. According to [13], the improvement in the mechanical properties can be caused by the solid-solution hardening induced by the substitution of neodymium atoms for nickel or aluminum atoms (this is thought to be unlikely, since the neodymium atomic radius is very large (0.182 nm)), the formation of segregations along grain boundaries, the removal of grain-boundary impurities (increase in the cohesion of grains), and structure refinement. The authors of [13] also note that, at high contents in NiAl alloys, REMs form compounds with both nickel and aluminum.

EXPERIMENTAL

We studied VKNA-type alloys with various compositions of the main and alloying elements (see table). As additional AEs, we used high-active (≤0.05 wt % Zr) and surface-active (0.015, 0.1, 0.2, 0.3 wt % La or La + Y) metals. The impurity contents in the alloys were no more than (wt %) 0.005 S, 0.015 P, 0.003 Sb, 0.5 Fe, 0.0005 Bi, 0.003 Sn, 0.001 Pb, 0.4 Si, and ≤0.015 O (the impurity contents were determined in every tenth heat).

The alloys were melted in a vacuum induction furnace with a base lining. Single crystals 16 m in diameter and 180 mm in length were grown by DS in UVNK-9 and UVNS-4 setups. Their orientation was ⟨111⟩; the deviation from the growth direction was ≤10°; and the block misorientation was ≤6°. We chose the ⟨111⟩ orientation using the fact that ⟨111⟩ crystals have the highest hot strength among the γ′-Ni_3Al-based intermetallic alloys [14]. In the alloys of type 1, lanthanum was introduced during the casting and DS of rods in the UVNS-4 setup. In the alloys of type 2, lanthanum was introduced from a NiLa master alloy during melting in the vacuum induction furnace.

The structure and phase states of the single-crystal samples of the Ni_3Al-based cast alloys grown by DS were studied by transmission electron microscopy (TEM), scanning electron microscopy (SEM), X-ray diffraction (XRD), X-ray phase analysis (XPA), electron-probe microanalysis (EPMA), and optical microscopy on a scanning electron–ion Quanta 200 3D microscope equipped with a Pegasus 2000 integrated system for microanalysis, a LEO 430 device, an EM-125 transmission electron microscope, a DRON-1.5 X-ray diffractometer (using CuK_α radiation), and a Neophot-32 (Atlas program) optical microscope. XPA can detect phases whose content is higher than 3–5 vol %, whereas TEM can identify phases that are present in a material at any (low) content.

RESULTS AND DISCUSSION

As was found in [15, 16], a VKNA-1B-type alloy has a complex phase composition and several structural constituents. Such an alloy contains primary γ′-Ni_3Al precipitates in the form of irregular (lily-like) particles 10–70 μm in size. The structure of these primary γ′-Ni_3Al precipitates is complex: in some cases, they contain spherical inclusions consisting of either *MC*-type refractory carbides or *MO*-type oxides around which the shells of nonequilibrium β-NiAl precipitates, which, in turn, serve as the nucleation centers of primary γ'_I precipitates, form. Moreover, the latter precipitates have a variable composition, which is supported by the data in [17]; therefore, we designate them as γ'_I and γ'_{II}. The primary γ′-Ni_3Al precipitates form rows or chains extended in the solidification direction and located in the interarm space. The interarm spacing is 150 μm. The dendrites have a eutectic origin and are based on the γ′ (γ'_{III}) phase, which contains isolated γ-phase (nickel-based solid solution with a random bcc structure) layers 0.6 μm thick.

Figures 1a and 2 show the typical microstructures of alloy 1 with various lanthanum contents after DS and annealing at 1000°C for 25 h. The compositions of the main phases were determined by EPMA on a LEO 430 device.

An analysis of the distribution of the main AEs in the main phases detected at a magnetization of ×3000–5000 demonstrates that, irrespective of the lanthanum content in the alloy (0.1 or 0.3 wt %) and the state of the

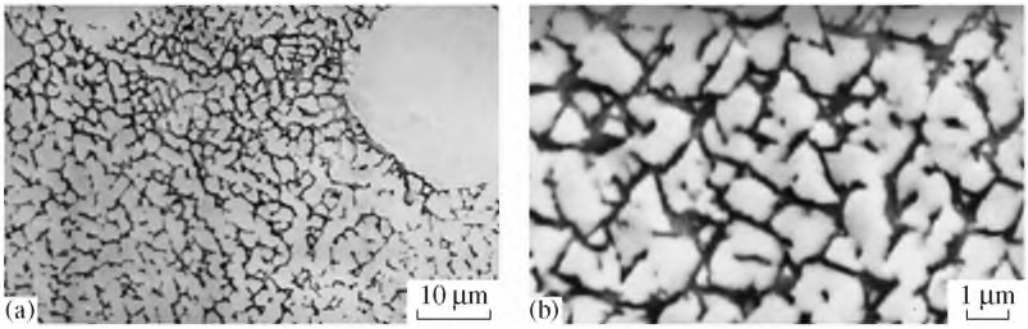

Fig. 1. Typical microstructures of intermetallic alloys of type (a) 1 and (b) 2 with 0.015 wt % La in the DS state.

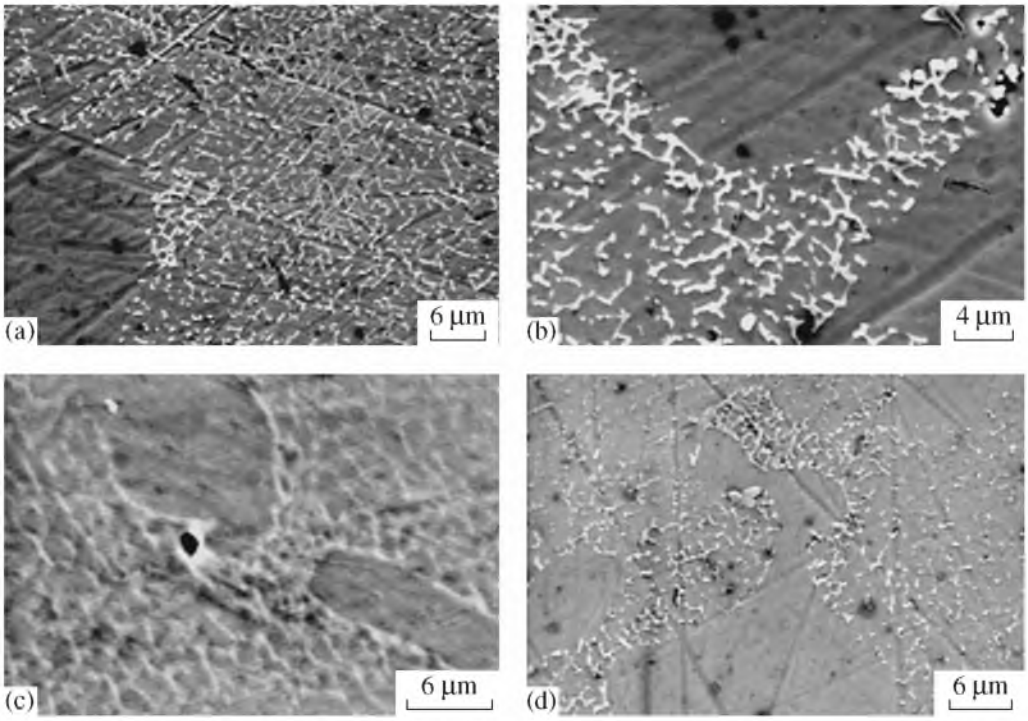

Fig. 2. Microstructures of alloy 1 with (a, b) 0.1 and (c, d) 0.3 wt % La in the states after (a, c) DS and (b, d) annealing at 1000°C for 25 h.

sample (after DS or annealing at 1000°C for 25 h), different regions in coarse primary γ'-Ni_3Al precipitates have somewhat different compositions and, hence, are conventionally designated as γ'_I and γ'_{II}. They are enriched in aluminum (14.39–14.95 at %) and titanium (2.60–2.82 at %) and contain chromium (3.67–3.84 at %), molybdenum (1.01–1.11 at %), and tungsten (0.71–0.75 at %). As follows from their composition, the γ'-Ni_3Al precipitates have a eutectic origin (γ'_{III}), and the layers in them consist of the γ-Ni solid solution; that is, in contrast to the compositions of γ'_I and γ'_{II}, they have lower contents of aluminum and all alloying elements ((in at %) 13.8 Al, 2.4 Ti, 3.3 Cr, 0.9 Mo, 0.65 W). The precipitates of the nickel-based γ solid solution are depleted of aluminum and titanium (~10 at % Al, ~1.2 at % Ti), and the contents of all other AEs in them are higher (~6 at % Cr, ~2.5 at % Mo, ~1 at % W).

A similar situation takes place in the case of the main phases in alloy 2 additionally alloyed with rhenium and cobalt (Fig. 1b). The precipitates of the γ' phase of various origins in alloys with 0.015 and 0.2 wt % La are enriched in aluminum and titanium, whose contents vary over wide limits, namely, 13.42–15.06 at % Al and 1.53–2.02 at % Ti. The contents of other AEs also vary over wide limits: 3.03–3.83 at % Cr, 1.76–2.80 at % Mo, 0.6–0.9 at % W, 3.03–3.94 at % Co, and 0.35–0.40 at % Re. The layers of the nickel-based γ solid solution are depleted of aluminum and titanium (~10 at % Al, ~1.1 at % Ti), and the contents of all other

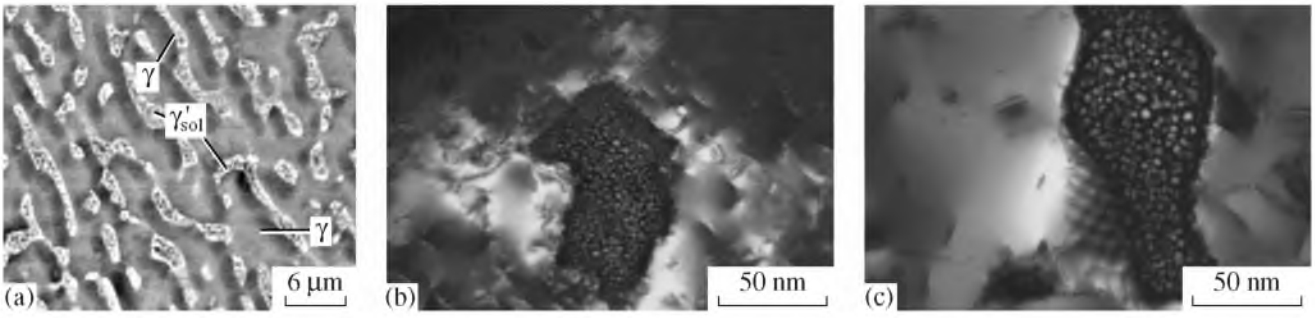

Fig. 3. Microstructures of alloy 1 with (a) 0.015, (b) 0.1, and (*c*) 0.3 wt % La. Particles of secondary γ'_{1V} (γ, γ'_{sol}, γ') precipitates are visible in alloy samples after (a) annealing at 1200°C for 4 h and (b, c) service-life tests at 1000°C and a stress of 150 MPa. (a) SEM and (b, c) TEM.

AEs in them are higher (7.5–8.8 at % Cr, 2.5 at % Mo, 5 at % Co, 0.7–1.2 at % Re).

When studying the alloy 1 DS samples subjected to a service-life test at 1000°C and a stress of 150 MPa by TEM, we detected γ'_{1V} precipitates (secondary precipitates from the supersaturated nickel-based γ solid solution), which form during the test and represent fine equiaxed particles 10–30 nm in size (Figs. 3b, 3c). In [1–3, 18], such γ'_{1V}-phase precipitates of larger sizes (70–150 nm) were detected in a DS alloy of type 1 in γ-Ni layers after high-temperature annealing at 1200°C (Fig. 3a). It is generally agreed that the formation of γ'_{1V} nanoparticles in the structure of alloys during high-temperature tests leads to the precipitation hardening of the γ structural constituent and to the additional hardening of the alloys. The composition of the γ'_{1V} nanoparticles was not determined because of their small sizes. It should be noted that the structure of the γ layers is similar to the structure of Ni superalloys. The main difference consists in the fact that this structure forms in intermetallic alloys upon high-temperature (1000–1200°C) annealing or long-term tensile tests. In Ni_3Al-based alloys, secondary γ'-phase precipitates (γ'_{1V} particles) are finer, whereas the γ' phase in Ni superalloys dissolve in the γ matrix at these temperatures (the structure degrades). As a result, these alloys are softened, and their working temperatures are limited.

An analysis of the energy dispersive spectra recorded from different areas of the polished sections of samples with 0.015, 0.1, and 0.3% La in the states after DS and annealing at 1000°C for 25 h and an analysis of the compositions of some large particles of the phases additional to the main $\gamma' + \gamma$ phases demonstrate that the alloys contain both nano- and microparticles of phases enriched in refractory bcc metals (Cr, Mo, W) and phases containing REMs (La, La + Y).

BCC Phase

As noted above, the dendrite arms in the DS structure in the cast material are enriched in refractory tungsten and rhenium, and the interarm space is enriched in elements with a lower melting temperature (e.g., titanium). The distributions of chromium and molybdenum over dendrite arms and the interarm space are the same; however, these atoms tend to segregate and to form phases with variable contents of chromium, molybdenum, tungsten, nickel, and AEs. According to ternary phase diagrams, these independent phases should represent α-(Cr, Mo, W) bcc solid solutions[3]. However, we failed to detect these phases in the cast state of the alloy even at high magnifications. In the absence of REMs (<0.0015 wt %) in the DS alloys (natural eutectic CMs), coarse microparticles of the following phases of variable composition can form: $Ni_{67}Al_{10}Ti_{1.5}Cr_{15}Mo_5W_1Re_{0.5}$ or $Ni_45Al_4Ti_1Cr_{35}Mo_{14}W_1$ (Fig. 4a). In alloys with 0.1–0.2 wt % La, nanoparticles form and additional hardening is provided by the nanoparticles (100–250 nm) of a phase of variable composition (with variable chromium, molybdenum, tungsten, nickel contents) and enriched in molybdenum, tungsten, and chromium. This phase was also detected in the presence of REMs in multicomponent Ni–Al–Cr–Mo–W–AE alloys [1], and it is absent in ternary Ni–Al–Mo(Cr) alloys. Thorough X-ray diffraction analysis of alloys with 0.3 wt % La revealed that this phase has an α-Mn-type crystal lattice with the space group $I43m$ and a lattice parameter a = 0.8856–0.9200 nm. Nanoparticles of this phase form upon annealing at 1000°C for 10–25 h at γ'/γ interfaces between primary γ'-Ni_3Al precipitates and a two-phase eutectic $\gamma' + \gamma$ region (Fig. 4b). Such precipitates were not detected in the as-cast state of the DS alloy.

Nickel, Aluminum, and Carbon Lanthanides

Our studies demonstrate that the DS alloys (natural eutectic CMs) with REMs undergo additional hardening by fine precipitates (1–2 vol %) of the lanthanides

[3] See footnote 2.

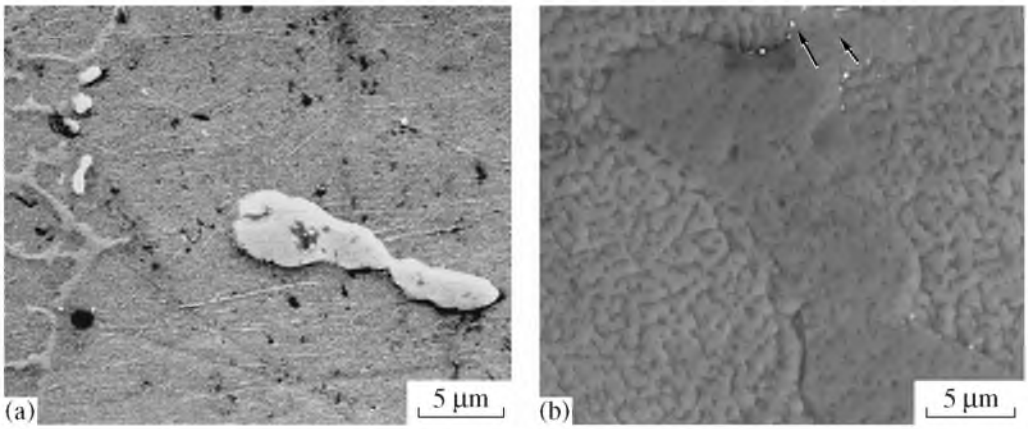

Fig. 4. Particles of the phase enriched in tungsten, molybdenum, chromium, and titanium in alloy 1: (a) sample without REM after annealing at 1200°C for 4 h and (b) sample with 0.1% La after annealing at 1000°C for 10 h.

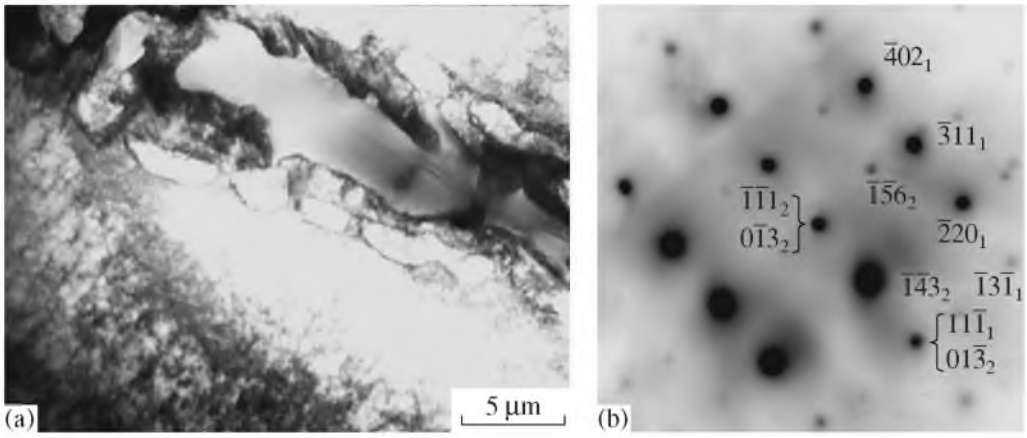

Fig. 5. Electron-microscopic image of a mixture of nickel and aluminum aluminides in alloy 1 with 0.3 wt % La annealed at 1000°C for 10 h: (a) bright-field image and (b) electron diffraction pattern with a key pattern.

Al_2La (space group $Fd3m$) and Ni_xLa_y. These lanthanides are detected in the cast material after DS, annealing at 1000°C for 10 h (Fig. 5), or long-term tests at 1000°C. According to the ternary Ni–Al–*R* phase diagrams, these lanthanides cannot be in equilibrium with nickel aluminides, since the field between them is closed by the La(Y, Ce)Ni_5 solid solution (in which aluminum substitutes for nickel) penetrating deep into the ternary system. Based on these studies of the alloys and the data on multicomponent NiAl-based alloys, we [18] proposed that the equilibria in the multicomponent Ni–Al–(Cr, Mo, W, Ti)–*R* systems (alloys) with other alloying elements shift and that phases that are not in equilibrium with nickel aluminides in simpler ternary phase diagrams can appear.

We also effected additional hardening by lanthanum carbide La_2C_3 (space group $I43d$) nanoprecipitates (10–20 nm) that form on dislocations in the γ-Ni solid solu-

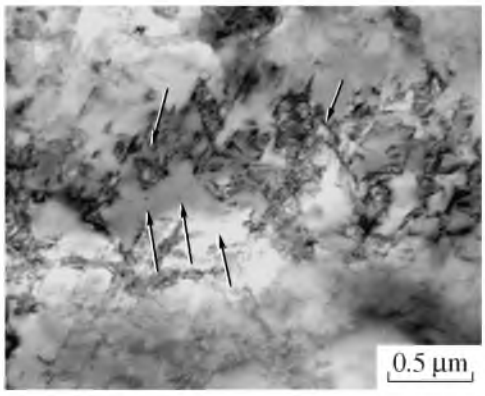

Fig. 6. Fine structure of alloy 1 annealed at 1000°C for 10 h. Carbide La_2C_3 particles (indicated by arrows) are located at dislocations.

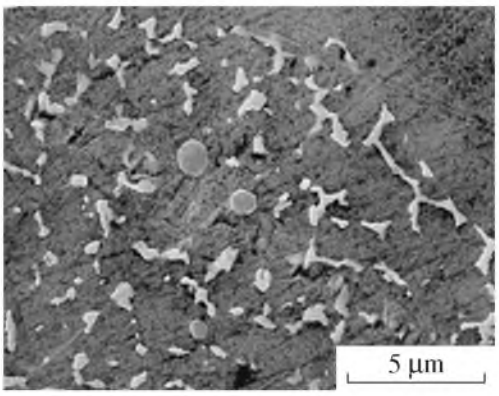

Fig. 7. Oxides in VKNA-1V alloy with 0.3% La after DS.

tion (Fig. 6). The La_2C_3 carbide appears in alloys with 0.3 wt % La and is not detected at lower concentrations.

Apart from these phases, the structure of the alloys contains coarse spherical inclusions, which are likely to be oxides (Fig. 7); they do not affect the structure and mechanical properties of the alloys.

These micro-, submicro-, and nanoparticles, which are enriched in chromium, molybdenum, and tungsten and have a variable composition and a random α-Mn-type bcc structure, and the Al_2La and Ni_xLa_y lanthanides stabilize the dendritic structure of the cast material to near-melting temperatures. We also implemented additional hardening of the γ-Ni solid solution by lanthanum carbide La_2C_3 nanoprecipitates (10–20 nm) forming on dislocations.

When studying the fine structures of both alloys, we did not find compounds of REMs with either sulfur or silicon. It should be noted that the introduction of REMs into Ni_3Al-based alloys does not change the total oxygen or sulfur content in them. However, the fixation of oxygen into spherical lanthanum (and yttrium) oxide particles provides oxygen redistribution in castings and removes it from grain boundaries.

Thus, alloying with refractory and rare-earth metals ensures the formation of nanophases in Ni_3Al-based alloys that stabilize the dendritic or single-crystal structure of VKNA-type DS cast alloys and strengthen the interface boundaries in them. In our next work, we will study the effect of alloying by REMs on the sizes of the structural constituents and on the strength and hot-strength characteristics of Ni_3Al-based alloys.

CONCLUSIONS

(1) We considered the hardening mechanisms that occur in Ni_3Al-based alloys in the working-temperature range up to 1200–1250°C, which is higher than the working temperatures of Ni superalloys.

(2) We showed that the designed cast high-temperature next-generation materials that are based on the intermetallic compound Ni_3Al and low alloyed with refractory (W, Re, Mo, Cr) and reaction- and surface-active (REM, Ti, etc.) metals represent natural γ'- Ni_3Al + γ-Ni eutectic DS CMs whose structure does not degrade up to near-melting temperatures, in contrast to Ni superalloys.

(3) When analyzing the phase diagrams of REMs with the AEs and impurities that are present in NiAl- and Ni_3Al-based alloys, we revealed excess phases that can precipitate upon alloying.

(4) We demonstrated that the alloying of Ni_3Al-based alloys with refractory and rare-earth metals provides the formation of nanophases that stabilize the dendritic or single-crystal structure of VKNA-type DS cast alloys and strengthen the interface boundaries in them.

ACKNOWLEDGMENTS

This work was supported by a grant of the President of the Russian Federation (project no. MK-3328.2007.3), a grant of the scietific school (NSh-3904-2008.3), and the Russian Foundation for Basic Research (project no. 07-03-00291-a).

REFERENCES

1. K. B. Povarova and O. A. Bannykh, "Principles for Designing Intermetallic-Based Structural Materials," Materialoved., No. 2, 27–33 (1999); No. 3, 29–37 (1999).
2. K. B. Povarova, "Physicochemical Foundations for the Creation of Thermally Stable Alloys Based on the Aluminides of Transition Metals," Materialovedenie, No. 12, 20–27 (2007); No. 1, 60–67 (2008).
3. K. B. Povarova and O. A. Bannykh, "Analysis of the Principles of Designing Nickel Superalloys and High-Temperature Alloys Based on the Intermetallic Compound Ni_3Al (γ' Phase)," in *Proceedings of the International Conference on Kishkin's Ideas and Modern Materials Science, Moscow, Russia* (VIAM, Moscow, 2006), pp. 11–21.
4. K. B. Povarova, N. K. Kazanskaya, A. A. Drozdov, and A. E. Morozov, "Rare-Earth Metals (REMs) in Nickel Aluminide–Based Alloys: I. Physicochemical Laws of Interaction in the Ni–Al–REM and Ni_xAl_y–REM–AE (Alloying Element) Systems," Izv. Ross. Akad. Nauk, Ser. Met., No. 1, 58–64 (2008) [Russian Metallurgy (Metally), No. 1, 46–51 (2008)].
5. K. A., Jr., Gschneidner and F. M. Calderwood, "C–Y (Carbon–Yttrium)," Bull. Alloy Phase Diagrams, **10** (1), 564–568 (1986).
6. O. N. Carlson and W. M. Paulson, "The Yttrium–Carbon System," Trans. AIME **242**, 846–852 (1968).
7. *Phase Diagrams of Binary Metallic Systems: A Handbook*, Ed. by N. P. Lyakishev (Mashinostroenie, Moscow, 1996–2000), Vols. 1–3. [in Russian].
8. E. I. Gladyshevskiĭ and O. I. Bodak, *Crystal Chemistry of the Intermetallic Compounds of Rare-Earth Metals* (Vishcha Shkola, Lviv, 1982).
9. H. Okamoto, "Si–Y (Silicon–Yttrium)," J. Phase Equilib. **12** (3), 397–399.

10. V. E. Glushkova and E. K. Keller," On the Polymorphism of Lanthanum Oxide," Dokl. Akad. Nauk SSSR **152** (3), 611–614 (1962).
11. T. B. Massalskiĭ, *Binary Alloy Phase Diagrams* (Metals Park, Ohio, 1987).
12. R. P. Elliot, *Constitution of Binary Alloys, First Supplement* (McGraw-Hill, New York, 1965; Metallurgiya, Moscow, 1970).
13. W. L. Ren, J. T. Guo, G. S. Li, and J. Y. Zhou, "Effect of Nd on Microstructure and Mechanical Properties of NiAl-Based Intermetallic Alloy," Mater. Lett. **57**, 1374–1379 (2003).
14. V. P. Buntushkin, K. B. Povarova, O. A. Bannykh, et al., "Effect of the Crystallographic Orientation on the Mechanical Properties of Single-Crystals of Alloyed Intermetallic Compound Ni_3Al," *Izv. Ross. Akad. Nauk, Ser. Met.*, No 2, 49–53 (1998).
15. K. B. Povarova, V. P. Buntushkin, O. A. Bazyleva and N. K. Kazanskaya, "Effect of the Structure on the Mechanical Properties of an Alloyed Ni_3Al Intermetallic Compound," Izv. Ross. Akad. Nauk, Ser. Met., 1995, No. 3, pp. 74–80
16. V. E. Efimov, "Effect of the Temperature–Time Treatment of the Melts of Ni_3Al-Based Intermetallic Alloys on Their Phase Composition and Hot Strength," in *Aviation Materials and Technologies. Ser. Ultrahigh-Temperature Materials for Modern and Promising Gas-Turbine Engines and Progressive Processes of Their Production* (VIAM, Moscow, 2003), pp. 79–92.
17. É. V. Kozlov, E. L. Nikonenko, N. A. Koneva, and N. A. Popova, "Morphology of the γ' Phase in Ni_3Al-Based Alloys," Deformatsiya i Razrushenie, No. 3, 44–47 (2006).
18. K. B. Povarova, A. A. Drozdov, V. P. Buntushkin, et al., "Effect of the Structural Stabilization by Nanoprecipitates and Disperse Precipitates of Phases Containing Refractory and Surface-Active Metals on the Properties of Ni_3Al-Based Alloys," in *Proceedings of the II International Conference on Deformation and Fracture of Materials and Nanomaterials, Moscow, Russia* (Interkontakt Nauka, Moscow, 2007), pp. 288–289.